

Development of an Analytical Model for Calculating the Stress Distribution of a Strip via the Roll Forming Process

Yonghui Park*, Changwoo Lee**,*** and Wei Shi****

Keywords: Roll forming, Flower pattern, Analytical model, Plane development, Cyclic loading.

ABSTRACT

Roll forming is a sheet metal forming process and is being increasingly used in the oil industry to mine crude oil. As mining regions experience unfavorable conditions, such as high pressures, corrosion, and cold, the quality of steel pipes needs to be guaranteed by improving the roll forming process. Several analytical models have been developed to determine the stress-strain distribution during forming. By assuming that the cross-section of the strip at each roll stands as a single plane, the strain distribution of the strip during the flower pattern stage was derived to observe the local deformation. Most of them does not consider the strain and stress distributions together or the advanced estimations including cyclic hardening due to loading and unloading process. In this work, a novel analytical model for calculating the strain distribution was integrated with the stress calculation model, which includes a cyclic hardening model. Moreover, the stress-strain results at each roll stand can be shown by developing the post-processing code to show how the internal status of the strip briefly. By using the model, the fact that the stress distribution and yield conditions are different was proven when the flower pattern was different.

Paper Received October, 2021. Revised July, 2022. Accepted April, 2023. Author for Correspondence: Dr. Wei Shi.

* Assistant professor, Department of Mechanical Engineering, Sunmoon University, Asan, Chungnam, Republic of Korea

** Principal researcher, Steel-pipe Technology Team, Pohang Institute of Metal Industry Advancement, Pohang, Kyungbuk, Republic of Korea

*** Department of Mechanical Engineering, Pohang University of Science and Technology, Pohang, Kyungbuk, Republic of Korea

**** Associate professor (Corresponding author), State Key Laboratory of Coastal and Offshore Engineering, Dalian University of Technology, Dalian, China

INTRODUCTION

The roll forming process forms a strip into a pipe form while passing through a series of forming rolls. In South Korea, this process has been applied to produce oil pipes for export to North America using the electric resistance welding (ERW) bonding method (Kang, 2012) (Fig. 1). The process involves various physical phenomena with many variables, which makes it difficult to analyze the relationships among the variables. As a result, most domestic pipe companies have applied a mass production method with small items that are required by certain global markets and major customers. However, due to the depletion of energy resources, petroleum production in severe environments, such as deep seas and extreme regions, demands high-quality and high-strength steel pipe products. In addition, in the aftermath of world protectionism, it has become difficult to supply large quantities to major customers (Rhee et al. 2018; Kang, 2015). In this situation, the steel pipe industry is sympathizing with the necessity of R&D investment to secure a new demand market, strategic approaches to the existing demand market, and high value-added products (Choi, 2019).

To ensure the quality and diversification of steel pipes, the basic activities involve obtaining a basic model of the product formability and the relationship between the various variables in the roll forming process. The finite element method (FEM) is a powerful technique that can identify the internal stress and strain of a deformable body based on a numerical analysis. In particular, the utilization of the FEM is very high in the roll forming process, which contains nonlinear phenomena, such as elastic-plastic deformation of the material and contacts between bodies. Several works have been conducted to solve troubleshooting in the field by using commercial software, such as ABAQUS; Dassulat Systemes, France, DEFORM; SFTC, United states of America, Marc; MSC Software, United states of America, and PROFIL; UBECO, Germany. For instance, types of thin-walled products formed by the roll forming process include the forming analysis of a hydroforming steel pipe (Lee, 2003) and the strength

evaluation of automobile parts, which is composed of high tensile strength steel sheets (Kim et al. 2010). Regarding the design of the process, evaluations of the stress on the strip when production variables, such as the roll-to-roll distance, roll gap, and the number of roll passes, change in the process have been conducted (Yoon et al. 2015; Kima et al. 2016; Kimb) et al. 2016). In addition, the FEM is widely used for the plastic deformation of various methods, such as uing-ouing-expansion (UOE) and 3-point bending (Yi et al. 2017; Kim et al. 2017). However, the FEM has the disadvantage of requiring much experience and skill of the interpreter and investment in computational environments. Additionally, domestic industries that are accustomed to developing a product through facility investment and testing of the roll forming process have difficulty using the process design because the FEM has difficulty providing results immediately. To overcome this problem, several models have been developed that can confirm product formability in the field by developing an analytical model customized for each manufacturing method (Fu et al. 2013). In particular, the flower pattern diagram was investigated by developing analytical models (Abeyrathna et al. 2016; Abeyrathna a) et al. 2017; Abeyrathna b) et al; 2017). In these works, the cross-section of the strip at each roll stand is assumed to be on a single plane, and the stress on the strip is calculated based on the strain due to the forming path or trajectory of a point at the edge of the strip during forming. However, these models do not consider the hardening phenomenon caused by cyclic loading on the strip. Based on this limitation, it is difficult to develop an analytical model that can simulate a three-dimensional nonlinear ERW tube process. However, if an analytical model is developed based on the development of a basic model and is then distributed to the field, and if an engineer can easily utilize it, it can then be a good tool to immediately check the product formability and reflect it in the process design.

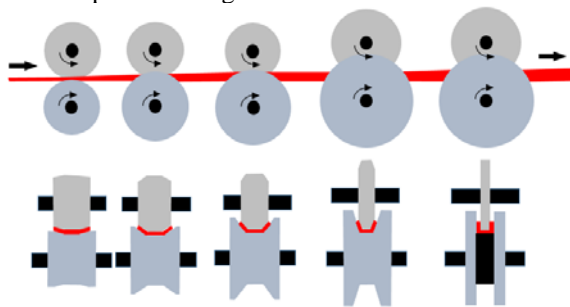


Fig. 1. Roll forming process.

In this study, we developed an analytical model that calculates the internal stress of the strip based on the flower pattern on the two-dimensional cross-section of the strip. The internal stress on the strip is calculated by mathematically expressing the change in the strain occurring at any position of the

cross-section and substituting it into the elastic-plastic and cyclic hardening material properties model. The model was also developed to include post-processing, such as plotting the time history of the stress on any point and the yield condition, which can see whether the point is undergoing elastic or plastic deformation. The effectiveness of the model was confirmed by comparing the internal stress of the strip and checking several physical properties when different flower patterns were applied.

ANALYTICAL MODEL

Flower Pattern

Through the roll forming process, a strip is finally dried in a pipe after each forming stage. The stage is a set of upper and lower rollers along the longitudinal direction of the pipe. The deformation of the strip, which is based on a two-dimensional cross-section perpendicular to the longitudinal direction of the strip, results in the rectangular cross-section to the circle, which is referred to as the flower pattern (Fig. 2). Fig. 2 shows different flower patterns by using different shapes of the forming roll and arrangement. However, there is no difference between the initial shape of the strip and the final shape of the strip that is rolled into the pipe form. Even if there is a difference in the intermediate process of drying, the strip can be seen and there is no difference in the final shape of the strip. Based on this fact, the variation in the internal strain of the strip between the initial shape and the final shape is derived using a mathematical expression.

The method to calculate the variation of the internal strain is comparing the coordinates and the orientation of any element that is divided in the width direction and the thickness direction of the strip (Fig. 3). The first step is dividing the strip into internal elements between the initial shape and the final shape. At each stage coordinates are given in every element. By using this code, users can select the number of parts in the width direction and the thickness direction according to their computational ability. Fig. 3 shows the flower pattern that has 32 elements in the initial shape and the final shape by dividing the initial shape of the strip into 8 equal parts in the width direction and 4 equal parts in the thickness direction. Due to the rectangular shape of each element, each element of the initial shape and the final shape of the strip consists of 4 boundary points, and is $(N_w + 1) \times (N_t + 1)$. In the case of Fig. 3, N_w is 8 and N_t is 4. Eq. (1) shows the x - y coordinates of the i -th in the width direction and the j -th in the thickness direction of the boundary point in the initial shape. Eq. (2) shows the x - y coordinates of the i -th in the width direction and the j -th in the thickness direction of the

boundary point in the final shape.

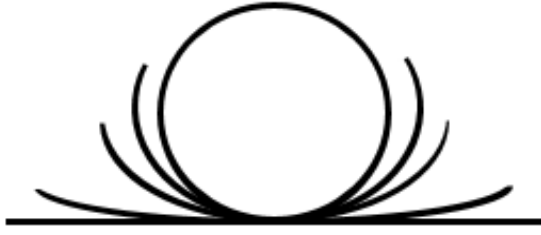


Fig. 2. Flower pattern.

$$x_{ini,i} = -\frac{l_w}{2} + \frac{l_w}{N_w} \times (i-1), \quad y_{ini,i} = -\frac{l_t}{2} - \frac{l_t}{N_t} \times (j-1) \quad (1)$$

$$x_{fin,i} = x_{ref} + r_j \times \cos(\theta_{i-1}), \quad y_{fin,i} = y_{ref} + r_j \times \sin(\theta_{i-1}) \quad (2)$$

where $i = 1, 2, 3, \dots, N_w+1, j = 1, 2, 3, \dots, N_t+1, l_w$ is the width length of the strip, l_t is the thickness length of the strip, x_{ref} and y_{ref} are the reference coordinates of the circle, r_j is the radius of the circle in the final shape, and θ_{i-1} is the angle of the circle with respect to the reference coordinates in the final shape.

Since it is difficult to define the coordinates of

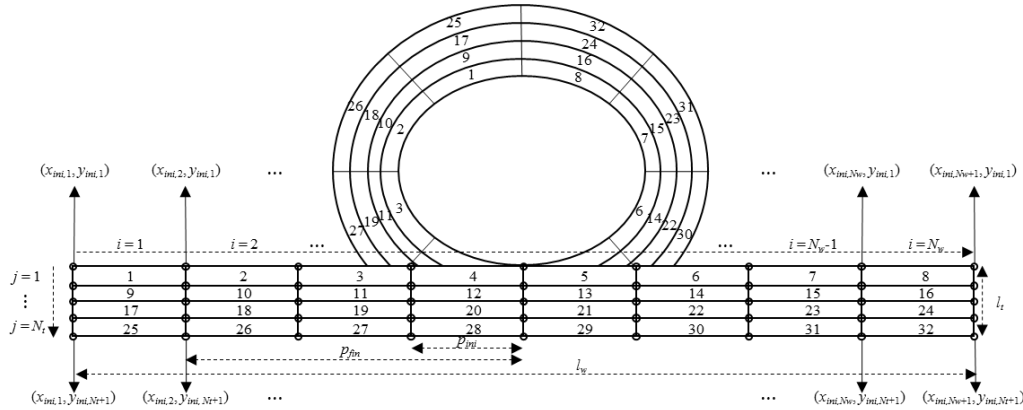


Fig. 3. Overview of the flower pattern and the number of elements.

$$xy_{ini,elem} = \left\{ \begin{array}{l} \left\{ \begin{array}{l} [x_{ini,1} \quad y_{ini,1}] \quad [x_{ini,2} \quad y_{ini,1}] \\ [x_{ini,1} \quad y_{ini,2}] \quad [x_{ini,2} \quad y_{ini,2}] \end{array} \right\} \quad \left\{ \begin{array}{l} [x_{ini,2} \quad y_{ini,1}] \quad [x_{ini,3} \quad y_{ini,1}] \\ [x_{ini,2} \quad y_{ini,2}] \quad [x_{ini,3} \quad y_{ini,2}] \end{array} \right\} \quad \dots \quad \left\{ \begin{array}{l} [x_{ini,N_w} \quad y_{ini,1}] \quad [x_{ini,N_w+1} \quad y_{ini,1}] \\ [x_{ini,N_w} \quad y_{ini,2}] \quad [x_{ini,N_w+1} \quad y_{ini,2}] \end{array} \right\} \\ \left\{ xy_{ini,elem,(N_w \times 1)+1} \right\} \quad \left\{ xy_{ini,elem,(N_w \times 1)+2} \right\} \quad \dots \quad \left\{ xy_{ini,elem,(N_w \times 1)+N_w} \right\} \\ \vdots \\ \left\{ xy_{ini,elem,(N_w \times (N_t-1))+1} \right\} \quad \left\{ xy_{ini,elem,(N_w \times (N_t-1))+2} \right\} \quad \dots \quad \left\{ xy_{ini,elem,(N_w \times (N_t-1))+N_w} \right\} \end{array} \right\} \quad (3)$$

$$xy_{fin,elem} = \left\{ \begin{array}{l} \left\{ \begin{array}{l} [x_{fin,1} \quad y_{fin,1}] \quad [x_{fin,2} \quad y_{fin,1}] \\ [x_{fin,1} \quad y_{fin,2}] \quad [x_{fin,2} \quad y_{fin,2}] \end{array} \right\} \quad \left\{ \begin{array}{l} [x_{fin,2} \quad y_{fin,1}] \quad [x_{fin,3} \quad y_{fin,1}] \\ [x_{fin,2} \quad y_{fin,2}] \quad [x_{fin,3} \quad y_{fin,2}] \end{array} \right\} \quad \dots \quad \left\{ \begin{array}{l} [x_{fin,N_w} \quad y_{fin,1}] \quad [x_{fin,N_w+1} \quad y_{fin,1}] \\ [x_{fin,N_w} \quad y_{fin,2}] \quad [x_{fin,N_w+1} \quad y_{fin,2}] \end{array} \right\} \\ \left\{ xy_{fin,elem,(N_w \times 1)+1} \right\} \quad \left\{ xy_{fin,elem,(N_w \times 1)+2} \right\} \quad \dots \quad \left\{ xy_{fin,elem,(N_w \times 1)+N_w} \right\} \\ \vdots \\ \left\{ xy_{fin,elem,(N_w \times (N_t-1))+1} \right\} \quad \left\{ xy_{fin,elem,(N_w \times (N_t-1))+2} \right\} \quad \dots \quad \left\{ xy_{fin,elem,(N_w \times (N_t-1))+N_w} \right\} \end{array} \right\} \quad (4)$$

each element as a simple matrix for the strain calculation using the difference between the initial shape and the final shape, the coordinates of the boundary point of each element, $xy_{ini,elem}$ and $xy_{fin,elem}$, were arranged as shell arrays that had 4 by 4 matrices in the location of each element, as shown in Eqs. (3-4).

In the coordinates of each element in the initial shape and the final shape of the strip shown in Eqs. (3-4), the same location means the same element, so the variation of the length and angle regarding the same element can be defined to predict the variation of the strain. To calculate the variation of the normal and shear strains, each element has a submatrix including geometric information, such as the length and angle of the element shown in Fig. 4. Each element has different deformation, so we need to classify the length and angle as a matrix in the specific space; shell matrix to calculate the normal and shear strain respectively. Eqs. 5-6 show the shell type of the matrix to have the geometric information in the initial shape and the final shape of the strip, respectively. This shell type has strength to match state variables such as the angle of the specific location during the deformation easily.

$$\Delta_{ini,elem} = \left\{ \begin{array}{l} \left[\begin{array}{ccc} \theta_{1,ini} & L_{1,ini} & \theta_{1,ini} \\ L_{4,ini} & L_{5,ini} & L_{2,ini} \\ \theta_{1,ini} & L_{3,ini} & \theta_{1,ini} \end{array} \right] \quad \Delta_{ini,elem,2} \quad \cdots \quad \Delta_{ini,elem,N_w} \\ \Delta_{ini,elem,(N_w \times 1)+1} \quad \Delta_{ini,elem,(N_w \times 1)+2} \quad \cdots \quad \Delta_{ini,elem,(N_w \times 1)+N_w} \\ \vdots \quad \vdots \quad \vdots \quad \vdots \\ \Delta_{ini,elem,(N_w \times (N_t-1))+1} \quad \Delta_{ini,elem,(N_w \times (N_t-1))+2} \quad \cdots \quad \Delta_{ini,elem,(N_w \times (N_t-1))+N_w} \end{array} \right\} \quad (5)$$

$$\Delta_{fin,elem} = \left\{ \begin{array}{l} \left[\begin{array}{ccc} \theta_{1,fin} & L_{1,fin} & \theta_{1,fin} \\ L_{4,fin} & L_{5,fin} & L_{2,fin} \\ \theta_{1,fin} & L_{3,fin} & \theta_{1,fin} \end{array} \right] \quad \Delta_{fin,elem,2} \quad \cdots \quad \Delta_{fin,elem,N_w} \\ \Delta_{fin,elem,(N_w \times 1)+1} \quad \Delta_{fin,elem,(N_w \times 1)+2} \quad \cdots \quad \Delta_{fin,elem,(N_w \times 1)+N_w} \\ \vdots \quad \vdots \quad \vdots \quad \vdots \\ \Delta_{fin,elem,(N_w \times (N_t-1))+1} \quad \Delta_{fin,elem,(N_w \times (N_t-1))+2} \quad \cdots \quad \Delta_{fin,elem,(N_w \times (N_t-1))+N_w} \end{array} \right\} \quad (6)$$

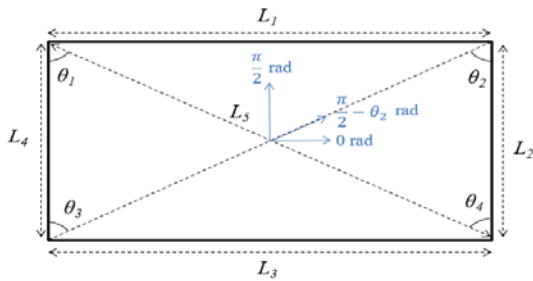


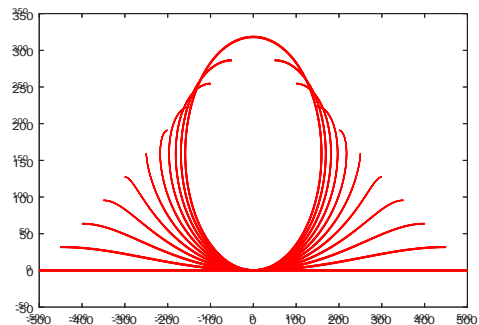
Fig. 4. The length and the angle of an element.

After calculating strains ϵ_1 , ϵ_2 , and ϵ_3 in the direction of 0 , $(\pi/2 - \theta_2)$ and $\pi/2$ from the center of the element, as shown in the blue marker in Fig. 4, Eqs. 7-8 calculate the normal and shear strains ϵ_x , ϵ_y , and γ_{xy} of the element by the strain transformation. Through these processes, the strain of each element in the plane can be obtained during the roll forming process from an initial rectangular shape to a final circular shape.

$$\begin{aligned} \epsilon_1 &= \frac{\epsilon_x + \epsilon_y}{2} + \frac{\epsilon_x - \epsilon_y}{2} \cos(2 \times 0 \text{ rad}) + \frac{\gamma_{xy}}{2} \sin(2 \times 0 \text{ rad}) \\ \epsilon_2 &= \frac{\epsilon_x + \epsilon_y}{2} + \frac{\epsilon_x - \epsilon_y}{2} \cos\left(2 \times \left(\frac{\pi}{2} - \theta_2\right) \text{ rad}\right) + \frac{\gamma_{xy}}{2} \sin\left(2 \times \left(\frac{\pi}{2} - \theta_2\right) \text{ rad}\right) \\ \epsilon_3 &= \frac{\epsilon_x + \epsilon_y}{2} + \frac{\epsilon_x - \epsilon_y}{2} \cos\left(2 \times \frac{\pi}{2} \text{ rad}\right) + \frac{\gamma_{xy}}{2} \sin\left(2 \times \frac{\pi}{2} \text{ rad}\right) \end{aligned} \quad (7)$$

$$\begin{bmatrix} \frac{1}{2} + \frac{1}{2} \cos(2 \times 0) & \frac{1}{2} - \frac{1}{2} \cos(2 \times 0) & \frac{1}{2} \sin(2 \times 0) \\ \frac{1}{2} + \frac{1}{2} \cos\left(2 \times \left(\frac{\pi}{2} - \theta_2\right)\right) & \frac{1}{2} - \frac{1}{2} \cos\left(2 \times \left(\frac{\pi}{2} - \theta_2\right)\right) & \frac{1}{2} \sin\left(2 \times \left(\frac{\pi}{2} - \theta_2\right)\right) \\ \frac{1}{2} + \frac{1}{2} \cos\left(2 \times \frac{\pi}{2}\right) & \frac{1}{2} - \frac{1}{2} \cos\left(2 \times \frac{\pi}{2}\right) & \frac{1}{2} \sin\left(2 \times \frac{\pi}{2}\right) \end{bmatrix} \begin{Bmatrix} \epsilon_x \\ \epsilon_y \\ \gamma_{xy} \end{Bmatrix} = \begin{Bmatrix} \epsilon_1 \\ \epsilon_2 \\ \epsilon_3 \end{Bmatrix} \quad (8)$$

However, the above processes are based on the difference between the initial shape and the final shape of the strip; they do not include the intermediate process of making a pipe. In other words, there is no change in the total strain of each element, but the intermediate process in which the position of the strip along the width direction is deformed at different speeds by each stage is not considered. Fig. 5 shows flower patterns with the different intermediate processes.



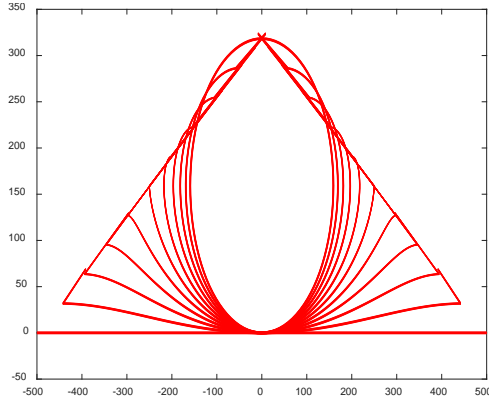


Fig 5. Comparison of different flower patterns.

In both cases there is no difference in the final shape compared to the initial shape, but the stress generated as the hysteresis experienced by each element varies. In particular, the quality of a product through plastic forming depends on the stress history due to the intermediate process. Since the flower pattern varies depending on the shape and arrangement of the shape of a forming roll, it is necessary to develop a mathematical model that can express the deformation history of the flower pattern and check the internal stress state.

To embody the deformation history of the arbitrary element from #1 to #32 in Fig. 3, we varied the slope to time of the strain function as the area under the slope to time of the strain function is constant. In other words, a simple strain rate model of the strip was developed to apply the relative strain rate for each element based on the target strain ϵ of each element that is the area of the function. In other words, different strain rates according to the width of the strip were applied to each arbitrary element to set the different intermediate processes for a fixed amount of time.

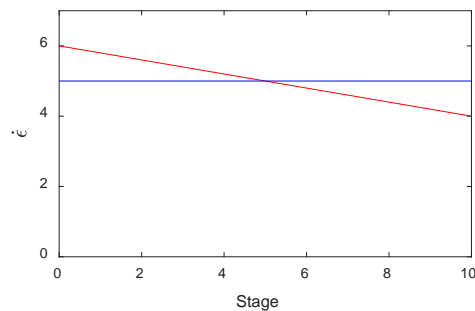


Fig. 6. Example of strain rate on an arbitrary element.

Fig. 6 shows the two different strain rates regarding the one of arbitrary elements from #1 to #32 in Fig. 3, where the area under the diagram represents the target strain. The final circular shape of the strip is derived only when the strain of all elements is changed by the target strain in a limited time, t_{end} . That is, when the

initial strain rate is determined, the final strain rate can be determined by calculating the area under the diagram and comparing the area to the target strain. Eqs. (9-12) derive the strain model over time by applying relative factors a and b to determine the relative strain rate in the initial and final states, respectively. This model will be used in the next section; Section Analysis - Calculation process to define the relative deformation speed referred to the reference speed v_r , corresponding to a and b , in the specific regions defined by users $p_{r,ini}$ to $p_{r,fin}$, referred to the center of the strip along to the width direction in Fig. 3.

The model cannot change the history of the target strain linearly, so it is difficult to represent the actual manufacturing process. In the future, we plan to develop a strain history model based on images of flower pattern deformation by assigning the coordinates of each element in the cross-section of the strip.

$$\frac{\dot{\epsilon}_{elem,ini} + \dot{\epsilon}_{elem,fin}}{2} \times t_{end} = \epsilon_{elem} \quad (9)$$

$$\frac{a \times \dot{\epsilon}_{elem,ref} + b \times \dot{\epsilon}_{elem,ref}}{2} \times t_{end} = \epsilon_{elem} \quad (10)$$

$$\dot{\epsilon}_{elem,ini} = \frac{\epsilon_{elem}}{t_{end}} \times \frac{2}{(a+b)} \quad (11)$$

$$\epsilon_{elem}(t) = \frac{a \times \dot{\epsilon}_{elem,ref} - b \times \dot{\epsilon}_{elem,ref}}{2 \times t_{end}} \times t^2 + b \times \dot{\epsilon}_{elem,ref} \times t \quad (12)$$

Strain-stress Transformation Model

A strain-to-stress transformation model was established based on the 3×3 strain tensor of each element obtained in the flower pattern process. The model was modified from the previous MATLAB code, which transforms strain to stress in the plane stress (Karolczuk, 2010). After calculating the 3×3 strain tensor of each element in every stage, the stress tensor of each element in every stage is calculated according to the stress-strain diagram created by the Ramberg-Osgood equation (Eq. 13). The developed model considers several elements that are divided into the first step, but the previous model only considers one element. About the coefficient of cyclic hardening K and the exponent coefficient of cyclic hardening n , these coefficients are determined by fitting the Ramberg-Osgood equation to the hardening behavior of the specific material measured stress-strain data.

$$\epsilon = \frac{\sigma}{E} + \left(\frac{\sigma}{K} \right)^{\frac{1}{n}} \quad (13)$$

Regarding the stress-strain model, the Hurber-Mises-Hencky test was used for the yield criterion, and an algorithm with the kinematic-isotropic hardening model that calculates the stress and back stress that changes according to the strain change via cyclic loading was used (Mróz. 1967; Garud. 1982; Karolczuk et al. 2006; Karolczuk. 2008).

We functionalized the previous model for only one element so that all the elements of the strip can undergo a strain-stress transformation. In other words, the strain in the current time is substituted into the transformation code in order to calculate the stress in the current time, and the stress in the current time is repeatedly used for the strain-stress transformation to calculate the stress in the next time.

ANALYSIS

Calculation Process

The program begins with the preprocessing process to determine the initial and final shapes as well as the deformation process of the strip. Then, it calculates the internal strain according to the flower pattern process and the strain-stress conversion process to give the internal stress distribution in each stage during post-processing (Fig. 7).

The main variables to be determined during preprocessing are the width and thickness of the strip. Additionally, the number of sections in each direction are divided to determine the total number of elements, and the divided section and speed difference must be entered in the width direction of the strip to consider the relative deformation speed of each element in the flower pattern deformation process (Table 1).

During post-processing, it is possible to obtain the stress distribution for every element and the stress history diagram for a specific element in the entire stage of the flower pattern. In particular, in the case of the stress history diagram the elastoplastic change and back stress experienced by the element can be confirmed via cyclic loading, thereby confirming the deformation state of the strip throughout the entire stage.

Table 1. Main variable to be determined in the pre-processing.

The initial and final shape	The relative deformation speed
w , Width	p_{rini} , the initial point of the section referred to the center of the strip along to the width direction
t , Thickness	p_{rfin} , the final point of the section referred to the center of the strip along to the width direction
N_w , The number of sections in the width direction	v_r , The relative deformation speed referred to the reference speed to apply from p_{rini} to p_{rfin} .
N_t , The number of sections in the thickness direction	

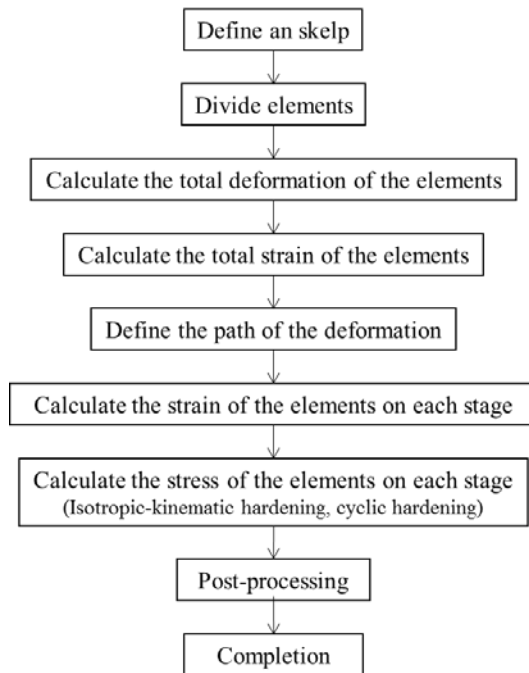


Fig. 7. Diagram of the calculation process for calculating the internal strain-stress of the flow pattern.

Simulation Condition

In the case of different flower pattern processes, to compare the stress distribution of the final shape of the strip, two simulations in which all sections of the strip are deformed at a constant speed in time (case 1) and are deformed at different speeds according to the width of the strip (case 2) are defined (Table 2). The elements that experienced different speeds, such as the strain rate, have different stress-strain curves compared to the other elements due to the nonlinear material properties, hardening status, and yielding conditions. The nonlinear material properties shown in Table 3 are applied to the two cases equally.

To easily see the difference, different speeds are applied to the edge of the strip. In other words, the edge of the strip is deformed rapidly at the beginning of roll forming and is deformed slowly as the strip approaches the final stage (Fig. 5). In addition to the stress distribution on all sections of the strip, an analysis regarding the internal quality of the strip was conducted to check whether the element was elastic-plastic, as well as the hardening status of the element.

Table 2. Simulation condition.

	Constant speed	Different speed
p_{rini}	0	1
p_{rfin}	1	1
v_r	1	2.3

Table 3. Material properties.

Property	Value	Property	Value
Young modulus, E	210 GPa	Poisson ratio, ν	0.3
Yield strength, σ_y	200 MPa	Coefficient of cyclic hardening, K	1,320
Maximum strength, σ_u	800 MPa	Exponent of cyclic hardening, n	0.2074

RESULTS AND DISCUSSIONS

Stress Distribution

When the strip was deformed at the same speed in all sections in the width direction, all elements exhibited the same stress distribution as they were bent at a constant curvature (Fig. 8). Based on the neutral axis of the circular strip in the final stage, the outer section is in tension and the inner section is in compression, with higher von Mises stress in the inner section. To examine the stress of each inner element in detail, the stress in the x -direction, which is the width direction of the strip, was the largest, and the stress in the y -direction, which is in the thickness direction and the shear stress in the x - y plane, were counted in terms of order of magnitude. In this way, as it is in the compressed state from the inside and in the tensile state from the outside, when all the forces are removed after roll forming is completed, all the elements are released in the opposite direction of the stress value, and the spring-back phenomenon occurs again. In other words, the current circular shape of the strip is not finished as the circular pipe, so it is further deformed to maintain the circular shape when a spring back occurs.

In Fig. 9, the history of the stress of three elements at the same position in the width direction but different positions in the thickness direction is shown based on the center of the strip. As described above, it can be seen that the history of the stress is different, depending on the location of the thickness. The relatively higher stress is derived at the inner section, and the lowest stress appears near the neutral axis. In addition, when this code is used, the stress distribution at each step can be checked together (Fig. 10).

Difference in the Von Mises Stress Distribution Along the Path of the Flower Pattern

Based on the simulation conditions indicated in Section Analysis – Simulation condition, the result of comparing the stress of the strip obtained by the constant strain rate and the relative strain rate shows a lower stress distribution in the relative strain rate in the final stage, even though it shows a higher stress distribution in the early stages (Fig. 11). When checking the stress history diagram, while many strains occurred in the early stages, in the second half the strains increased in other sections, resulting in

relatively low strain and cyclic deformation (Fig. 12).

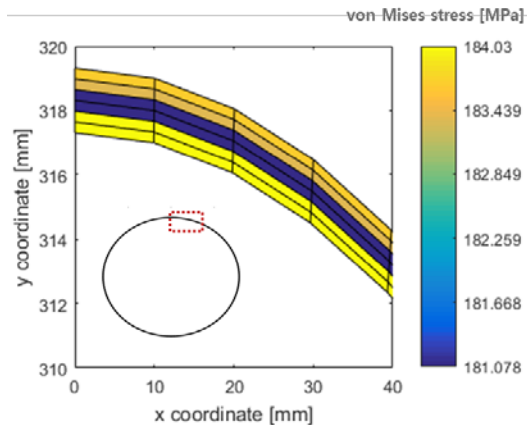


Fig. 8. Stress distribution of the final shape of the strip of the case 1.

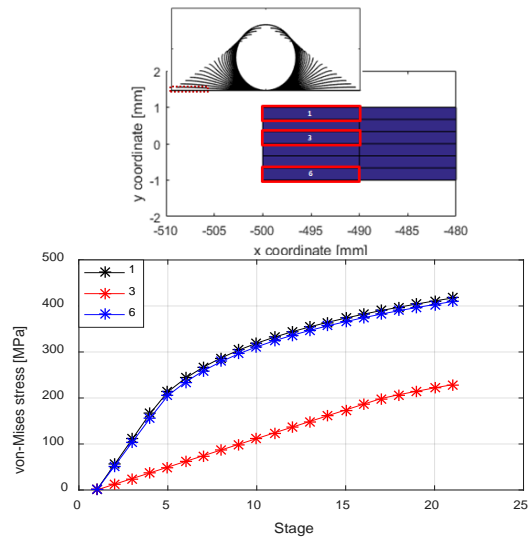


Fig. 9. History of stress distribution in each stage of the case 1.

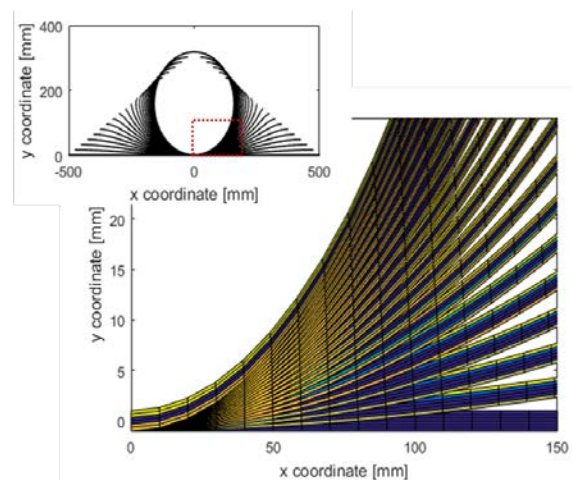


Fig. 10. Stress distribution in each stage of the case 1.

That is, as the force for deformation decreases, it goes down to elastic deformation from plastic deformation. Accordingly, Fig. 12 shows that the springback shape also acts as a cause due to the different internal stress distributions of the strip in the case of constant strain rate deformation and relative strain rate deformation. The code could not estimate the spring back, but since the internal stress value that may occur depending on the flower pattern process is derived, it is possible to confirm the possibility of model development and utilization.

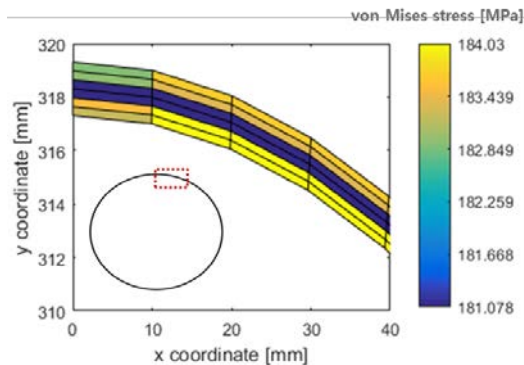


Fig. 11. Stress distribution of the final shape of the strip of the case 2.

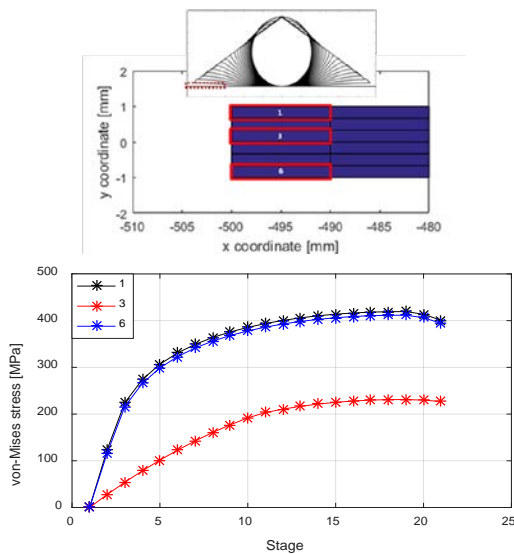


Fig. 12. History of stress distribution in each stage of the case 2.

CONCLUSIONS

The code for calculating the internal stress is developed by expressing the process of forming a pipe, in which a straight-type strip curls into a circular-type strip, as a two-dimensional analytic model. The code can be used as a predictive model for engineers to check the internal condition of strips according to the roll forming process by combining a

simple model that predicts the strain change of the flower pattern and a model that converts the strain to the stress of the strip. Using this model it can be confirmed that the internal stress is different when undergoing different flower pattern processes.

In the future, we will conduct a study that calculates and reflects the actual strain through coordinate assignments in the flower pattern, develops a deformation model corresponding to the actual flower pattern process, and takes 3D longitudinal deformation in 2D into account to improve the accuracy of the computational model.

DECLARATION OF CONFLICTING INTERESTS

The Authors declare that there is no conflict of interest.

ACKNOWLEDGEMENT

The authors thanks to Pohang Institute of Metal Industry Advancement, and Pohang University of Science and Technology(POSTECH) for their laboratory facilities, including the programming language; MATLAB. This work was supported by the Sunmoon University Research Grant of 2023. In addition, this research was partially funded by the National Natural Science Foundation of China (Grant No. 52071058) and LiaoNing Revitalization Talents Program (XLYC1807208).

REFERENCES

Abeyrathna, B., Rolfe, B., Hodgson, P., Weiss, M., “An extension of the flower pattern diagram for roll forming”; *The International Journal of Advanced Manufacturing Technology*, Vol. 83, No. 9, pp. 1683-1695(2016).

Abeyrathna^{a)}, B., Rolfe, Weiss, B. M., “The effect of process and geometric parameters on longitudinal edge strain and product defects in cold roll forming”; *The International Journal of Advanced Manufacturing Technology*, Vol. 92, No. 1, pp. 743-754(2017).

Abeyrathna^{b)}, B., Rolfe, B., Hodgson, P., Weiss, M., “Local deformation in roll forming”; *The International Journal of Advanced Manufacturing Technology*, Vol. 88, No. 9-12, pp. 2405-2415(2017).

Choi, J. W., “Korean Iron & Steel Association News”; Korea iron & steel association, Seoul, Korea(2019).

Fu, Z., Tian, X., Chen, W., Hu, B., Yao, X.,

- “Analytical modeling and numerical simulation for three-roll bending forming of sheet metal”; *The International Journal of Advanced Manufacturing Technology* Vol. 69, No. 5-8, pp. 1639-1647(2013).
- Garud, Y., “Prediction of stress-strain response under general multiaxial loading”; Proc., of Mechanical Testing for Deformation Model Development - ASTM International, West Conshohocken (1982).
- Kang, H. W., “Technology development trend of oil pipe (ERW pipe manufacturing technology)”; *Trends in Materials & Material Engineering*, Vol. 25, No. 6, pp. 57-64(2012).
- Kang, M. J., “Study on the Consistency of the United States Antidumping Measures against Korean OCTG with WTO Rules - Focused on analysis of Anti-dumping agreement 2.2.2.”; *Soongsil Law Review*, Vol. 33, pp. 1-28(2015).
- Karolczuk, A., Łagoda, T., Ogonowski, P., “Verification of low cycle fatigue energy-based criteria for metals”; *Politechnika Opolska, Studia i monografie*, Vol. 186, pp. 109(2006).
- Karolczuk, A., “Non-local area approach to fatigue life evaluation under combined reversed bending and torsion”; *International Journal of Fatigue*, Vol. 30, No. 10-11, pp. 1985-1996(2008).
- Karolczuk, A., “Strain2Stress - MATLAB Central File Exchange”; Mathworks, Boston, The United States of the America (2010).
- Kim, D. K., Cho, K. R., Park, S.E., Lee, K. H., Moon, Y. H., Lee, M.Y., “The Study of Manufacturing Technology for Front Bumper Beam with Roll Forming Process”; Proc., of the Korean Society for Technology of Plasticity Conference, Seoul 2010.
- Kim^{a)}, D. H., Jung, D. W., Nguyen, H. T., “Study of forming analysis of high tension steel according to roll gap in 30-pass roll forming process”; Proc., of the Korean Society of Manufacturing Technology Conference, Seoul, 2016.
- Kim^{b)}, D. H., Zhang, Y., Jung, D. W., “A Study of Spring-back Effect According to the Number of Roll Passes in the Roll Forming Process”; *Journal of the Korean Society of Manufacturing Process Engineers*, Vol. 15, No. 1, pp. 42-49(2016).
- Kim, K. W., Kim, T. B., Kim, M. K., Cho, W. Y., “An Analytical Model of Steel Pipe Forming Using Three Roll Bending”; Proc., of the Korean Society of Civil Engineers conference, Seoul, 2017.
- Lee, B. Y., “A Study on Roll Forming of Steel Pipe for Hydroforming”; Master thesis, Department of Mechanical Engineering, Korea Maritime University, Pusan, Korea(2003).
- Mróz, Z., “On the description of anisotropic workhardening”; *Journal of the Mechanics and Physics of Solids*, Vol. 15, No. 3, pp. 163-175(1967).
- Rhee, J. W., Park, E. K., “Interpretation and Adoption of Article 2.2.2 of WTO Anti-dumping Agreement - Focused on Issues Regarding to Calculation of Constructed Value in US-OCTG(Korea)(DS488)”; *Korean Journal of International Economic Law*, Vol. 16, No. 3, pp. 39-74(2018).
- Yi, J. W., Kang, S. C., Koh, H. M., “Prediction of Collapse Pressure of UOE Pipes using Pipe Forming Simulation”; Proc., of the Korean Society of Civil Engineers conference, Seoul, 2017.
- Yoon, D. H., Kim, D. H., Zhang, Y., Jung, D. W., “Study on the Effect of the Distance between the Rolls in the Roll Forming Process”; Proc., of the Korean Society for Technology of Plasticity Conference, Seoul, 2015.

NOMENCLATURE

- N_w The number of boundary points along the width
- N_t The number of boundary points along the thickness
- l_w The width length of the strip
- l_t The thickness length of the strip
- x_{ref}, y_{ref} The reference coordinates of the circle
- r_j The radius of the circle in the final shape
- θ_{i-1} The angle of the circle with respect to the reference coordinates in the final shape
- $xy_{ini,elem}, xy_{fin,elem}$ The boundary point of each element
- $\varepsilon_x, \varepsilon_y, \gamma_{xy}$ The normal and shear strains
- t_{end} The target strain in a limited time
- a, b The relative factors to determine the relative strain rate in the initial and final states
- $p_{r,ini}$ to $p_{r,fin}$, The specific regions referred to the center of the strip along to the width direction
- v_r The reference speed in the specific regions $p_{r,ini}$ to $p_{r,fi}$

通過輓壓成型工程計算帶材應力分佈的分析模型的開發

樸永輝 李昌宇 施偉
浦項科技大學

摘要

輓壓成型是一種金屬板材成型工藝，正被越來越多地應用於石油工業中的原油開採。由於開採區域存在高壓、腐蝕和寒冷等不利條件，需要通過改進輓壓成型工藝來保證鋼管的質量。已經開發了幾種分析模型來確定成形過程中的應力和應變分佈。通過假設每個輓的帶材橫截面都是單平面的，推導出了花紋預壓階段帶材的應變分佈以觀察局部變形情況。大多數模型不同時考慮應變和應力分佈，也沒有包括由於加載和卸載過程中迴圈硬化而產生的高階估計值。在本研究中，將用於計算應變分佈的新型分析模型與包含迴圈硬化模型的應力計算模型進行了集成。此外，通過開發後處理程式碼來展示每個輓位置的應力-應變結果，以簡要展示帶材的內部狀態。通過使用該模型，證明了花紋不同時應力分佈和屈服條件的差異。